Complex bacterial diversity of Guaymas Basin hydrothermal sediments revealed by synthetic long-read sequencing (LoopSeq)

John E. Hinkle[1], Jeffrey P. Chanton[2], Molly A. Moynihan[3,4], S. Emil Ruff[3,4], Andreas Teske[1*]

[1]Department of Earth, Marine and Environmental Sciences, University of North Carolina at Chapel Hill, Chapel Hill, NC, USA
[2]Department of Earth, Ocean and Atmospheric Science, Florida State University, Tallahassee, FL
[3]The Ecosystems Center, Marine Biological Laboratory, Woods Hole, MA
[4]The Bay Paul Center for Comparative Molecular Biology and Evolution, Marine Biological Laboratory, Woods Hole, MA

*** Correspondence:**
Andreas Teske
teske@email.unc.edu

Keywords: LoopSeq, 16S rRNA, sulfur-cycling bacteria, sulfur cycle, Guaymas Basin, hydrothermal sediments

Abstract. Hydrothermal vents host phylogenetically diverse and physiologically complex microbial communities. Previous studies of microbial community structure in hydrothermal sediments have typically used short-read sequencing approaches. To address these shortcomings, we use LoopSeq, a high-throughput synthetic long-read sequencing method that has yielded promising results in analyses of microbial ecosystems, such as the human gut microbiome. In this study, LoopSeq is used to obtain near-full length bacterial 16S rRNA gene sequences from hydrothermal sediments in Guaymas Basin. Based on these sequences, high-quality alignments and phylogenetic analyses provided new insights into the taxonomic diversity of sulfur-cycling microorganisms and their distribution along a lateral hydrothermal gradient. In general, LoopSeq-derived 16S rRNA gene sequences aligned consistently with reference sequences in GenBank; however, chimeras were prevalent in sequences as affiliated with the thermophilic *Candidatus* Desulfofervidus and *Thermodesulfobacterium*, and in smaller numbers within the sulfur-oxidizing family *Beggiatoaceae*. Our analysis of sediments along well-documented thermal and geochemical gradients show how sulfur-cycling bacteria of different taxonomic groups persist as active catalysts of the sulfur cycle in varying combinations throughout surficial hydrothermal sediments in the Guaymas Basin.

INTRODUCTION

The Guaymas Basin is a marginal rift basin in the Gulf of California that is characterized by the coexistence of hydrothermal vents and cold seeps. Unlike many other regions with hydrothermal vents, Guaymas Basin is subject to relatively high sediment accumulation rates and freshly emplaced basaltic sills drive the hydrothermal circulation of hydrocarbons, sulfide, and nutrient-rich fluids (Einsele et al. 1980, Lizarralde et al., 2011). This sustains highly active and very diverse microbial communities at the sediment surface (Teske et al., 2021). As a result, Guaymas Basin has been the subject of many sequencing studies throughout the past two decades, starting with the use of near-full-length (~1500bp) cloned PCR products (Teske et al., 2002) and progressed to high throughput pyrosequencing of very short (~80 bp) 16S rRNA gene fragments (Ruff et al., 2015). More recent studies utilize high throughput sequencing methods that produce longer (~400-500bp) 16S rRNA gene fragments (Teske et al., 2019, Su et al., 2023). The abundance of sequence data obtained via different methods makes the Guaymas Basin an ideal model system to assess the effectiveness of new next-generation sequencing technologies, such as LoopSeq. LoopSeq is a high-throughput synthetic long-read sequencing method (Callahan et al., 2021). Studies using clone library sequencing methods yield near full-length and high-quality sequences but are greatly limited by throughput and sequencing depth. Clone library-based methods are time consuming and only the most abundant microorganisms are usually detected . In turn, high throughput sequencing methods can yield tens of thousands of sequence reads, allowing to detect extremely rare organisms (Sogin et al., 2006). Yet, these reads are too short for high-resolution phylogenetic analyses and can only be used for relatively basic taxonomic identification. Short reads of 400-500 bp can be used to construct coarse phylogenies, but placement of unknown or poorly resolved lineages remains problematic, due to the limited information provided by short sequences and limited bootstrap support for phylogenetic branching patterns (Teske et al., 2019, Ramírez et al., 2021).

LoopSeq bridges this gap and allows to obtain nearly-full-length 16S rRNA gene sequences while performing high throughput, for the same cost as short read amplicons. This enables thorough diversity surveys of known microbial lineages, as well as high-resolution phylogenetic placement of rare or poorly resolved microbial lineages even at highly diverse ecosystems, such deep-sea hydrothermal sediments. To test the capabilities and reliability of LoopSeq for environmental samples, Guaymas Basin is ideal because i) the ecosystem is very well

understood, ii) the hydrothermal sediments are very diverse, iii) the sediments are rich in organics that can be problematic for sequencing, e.g. hydrocarbons, and iv) extensive 16S rRNA gene sequence databases are available for multiple habitats to verify LoopSeq sequences against short read and full-length sequence databases.

METHODS

Sampling. Guaymas Basin sites were visited and sampled with R/V *Atlantis*, HOV *Alvin*, and AUV *Sentry* during cruise AT37-06 (December 6-29, 2016). *Alvin* dives targeted previously explored sampling areas in the southern axial valley of Guaymas Basin (Teske et al., 2016), or newly identified sites found by AUV *Sentry*. Hydrothermal sediment samples (Alvin push cores) used in this study were obtained during Alvin Dive 4872 (Dec. 24, 2016) in the Cathedral Hill area (27.00.684 N/ 111.24.266 W) at 2014 m depth. The sample set covers a gradient from hot hydrothermal sediments covered with orange and white *Beggiatoaceae* mats to temperate bare sediment, within ~1 m distance (Fig. 1). Core 4872-01 is not covered by a *Beggiatoaceae* mat (bare sediment), Core 4872-06 is covered by a white *Beggiatoaceae* mat, and Core 4872-14 is covered by an orange *Beggiatoaceae* mat. Once returned to the surface, porewater profiles were collected using rhizons (Rhizosphere Research Products). Then, these cores were divided into 3 cm sections and methane samples were collected. The remaining sediment samples were frozen at -80°C by the shipboard science crew, and later used for DNA extraction shoreside.

Thermal profiles. Thermal profiles were measured in surficial sediments using *Alvin's* 50 cm heat flow probe (https://ndsf.whoi.edu/alvin/using-alvin/sampling-equipment/). The 50 cm probe contains thermal sensors every 10 cm, starting 5 cm below the attached plastic disc (the "puck") that limits probe penetration and rests on the seafloor once the probe was inserted. After 5 to 10 minutes of temperature reading stabilization, temperature readings were recorded**.**

Geochemical analyses. For sulfide analysis, 1 mL porewater subsamples were fixed with 0.1 mL of 0.1 M zinc acetate solution to preserve sulfide as zinc sulfide until analysis using the methylene blue method (Cline, 1969). For sulfate measurements, porewater samples were diluted in water (1:50) and analyzed using ion chromatography (Metrohm 930 Compact IC flex with Metrosep A PCC HC/4.0 preconcentration column, and Metrosep A Supp 5 Guard/4.0 chromatography column). Sulfate for the white and orange cores was measured by Wetland Biogeochemistry Analytical Services (WBAS) using ion chromatography on a Dionex ICS-1000

using a RFIC IonPac AS22 4 × 250 mm column and a RFIC IonPac AG22 Guard column 4 × 50 mm. The IC was calibrated using a 5-point standard curve and a minimum R^2 value of 0.999. The detection limit measured at 0.10 ppm sulfate. A check standard was made from a Dionex 7 anion standard (1000 ppm) to a concentration of 15 ppm. An external Standard from HACH (100 ppm sulfate) was used to make a 20 ppm quality check standard. In general, quality checks were analyzed for 10 % of the samples.

Porewaters from the Guaymas Basin were analyzed at WBAS for nitrate/nitrite (NO_x) and ammonium (NH_4^+) concentrations colorimetrically, using a Flow Solutions IV segmented flow Auto Analyzer from O.I Analytical, College Station, TX. The HCl-acidified samples were neutralized with sodium hydroxide (NaOH) before analysis. NO_x was determined using the cadmium reduction method and NH_4^+ was determined using the phenate method. Both nutrients were diluted to get their concentrations within the linear range of the auto analyzer. Quality control standards from certified stock standards (Environmental Research Associates), were analyzed every 15-20 samples.

For combined concentration and $\delta^{13}C$ analysis of methane, 2 mL sediment subsamples were added to 30 mL serum vials containing 2 mL of 1 M NaOH solution, sealed with thick butyl rubber stoppers, crimped with aluminum seals, and stored at 4°C. Since cores were retrieved unpressurized, outgassing may have impacted in particular the measurements of methane concentrations near and above saturation. After the cruise, the methane samples were analyzed by headspace gas chromatography-flame ionization detection (GC-FID) at Florida State University (Magen et al., 2014). Additionally, the gas samples were analyzed for $\delta^{13}CH_4$ by injecting 0.1 to 0.5 mL of sample into a gas chromatograph interfaced to a Finnigan MAT Delta S Isotope Ratio Mass Spectrometer inlet system as previously described (Chanton and Liptay 2000). Values are reported in the per mil (‰) notation relative to Vienna Pee Dee Belemnite (VPDB).

DNA extraction. DNA was extracted from Guaymas Basin sediment samples using a modified version of the protocol developed by Zhou et al., 1996 (see supplementary material). The extraction method was optimized for deep-sea sediments. The detailed protocol can be found in the supplementary materials.

LoopSeq sequencing. Sequencing libraries were prepared from extracted genomic DNA with the commercially available LoopSeq kits from Loop Genomics

(https://go.elementbiosciences.com/16s-loopseq-user-guide). Synthetic long reads (SLRs) were constructed from the short-read sequencing reads using the standard Loop Genomics informatics pipeline and processed as previously described (Callahan et al., 2021). The method involves attaching two DNA tags: one Unique Molecular Identifier (UMI) to each unique "parent" DNA molecule and one sample-specific tag (i.e., a sample index) equally to all molecules in the same sample. Barcoded molecules are amplified, multiplexed, and each UMI is distributed intramolecularly to a random position within each parent molecule. Molecules are then fragmented into smaller units at the position of each UMI, creating a library of UMI-tagged fragments with an average length of 400 bp compatible with an Illumina sequencing platform run in PE150 mode (Callahan et al., 2021).

This protocol allows for the assembly of continuous 16S rRNA gene long reads from individual DNA molecules, providing sequencing data like classical long read sequencing methods but with much higher throughput. Additionally, LoopSeq can be performed on existing DNA sequencing instruments, and due to the chemistry and the tagging of individual molecules the method is semi-quantitative providing a major advantage towards other amplification-based methods.

We note that LoopSeq reconstructs a single long read from several short reads. Therefore, we define the resulting amplicon sequence variants (ASVs) as LoopSeq variants (L-ASVs) to differentiate them from "traditional" ASVs that are essentially PCR amplicons.

DADA2 analysis. 16S rRNA gene sequences obtained by LoopSeq sequencing were analyzed using the DADA2 bioinformatics package available in R (Callahan et al., 2016) and LoopSeq suitable DAD2 workflow (Callahan et al., 2021). DADA2 creates ASVs (or LoopSeq variants (L-ASVs) in our case) by grouping together amplicon reads of the same sequence. Raw reads were transformed through primer removal, filtering, and denoising steps (Suppl. Table 1). Several levels of taxonomic resolution were tested to visualize the distribution of bacterial lineages present in our sediment samples. We found that higher levels of taxonomic resolution (e.g. Genus, Species) largely increased the number of unidentified sequences. Whereas lower levels of taxonomic resolution (e.g., Order) yielded a more satisfactory representation of bacterial diversity via the identification of clearly identified (often cultured) bacterial lineages.

16S rRNA gene sequence phylogeny. 16S rRNA gene sequences of microbes that are representative of the Guaymas Basin were obtained from the NCBI GenBank database and were

aligned using Multiple Sequence Comparison by Log-Expectation (MUSCLE) in MEGA11 (Stecher et al., 2020). From these alignments, MEGA11 was used to construct minimum-evolution phylogenetic trees checked by the aggregate of 1000 bootstrap replications (Rzhetsky & Nei, 1992, Felsenstein, 1985).

16S rRNA gene sequence distance matrices. Distance matrices corresponding to each phylogenetic tree are shown in the Supplementary Data File. The number of base substitutions per 100 sites from between sequences are shown. This displays the sequence identity data as a percentage. Analyses were conducted using the Maximum Composite Likelihood model (Tamura et al., 2004). Each analysis involved all 16S rRNA gene sequences displayed in the corresponding phylogenetic tree. All ambiguous positions were removed for each sequence pair (pairwise deletion option). Evolutionary analyses were conducted in MEGA11 (Tamura et al., 2021, Stetcher et al., 2020).

RESULTS AND DISCUSSION

Sediment characteristics. Temperature was measured in situ with the Alvin heat flow probe. Temperatures across mat-covered sediments guided the selection of sampling sites. The color of Guaymas Basin *Beggiatoaceae* mats indicated the temperature of the underlying sediment; orange mats covered hotter sediments and white mats covered comparatively cooler sediments (McKay et al., 2012).

Temperature varied greatly with increasing sediment depth at the three sample sites (Figs. 1 & 2a; Table 1). Temperatures at 40 centimeters below the seafloor (cmbsf) exceeded 100 ºC below the orange mat, reached 75 ºC below the white mat, and remained near 20 ºC in sediments without a *Beggiatoaceae* mat (Fig. 2a, Table 1).

Temperature considerably impacted microbial population density, and therefore the amount of DNA available for extraction. Measurable concentrations of DNA persisted the deepest (40 cmbsf) in Core 1, from bare sediment neighboring the warm mats. In contrast, DNA recovery is limited to surficial sediments (~ 20 cmbsf) in Core 14 from the hot center of the orange mat (Fig. 2b., Table 1). Interestingly, the highest DNA yields are found within the upper ~6 cm of sediment in all three cores, indicating that the impact of hydrothermal activity extends to the bare sediments of Core 1 (Fig. 2b, Table 1). Previous research in Guaymas Basin consistently reveals a very rapid decline in cell counts and 16S rRNA gene abundances with

increasing depth and temperature in hot hydrothermal sediments (Meyer et al., 2013, Møller et al., 2018, Lagostina et al., 2021).

Relatively low concentrations of sulfide are observed throughout the bare sediment core, whereas the white and orange mat cores have noticeable concentrations of sulfide (Fig. 2c, Table 1). At the surface, sulfide levels are near zero for the bare sediment and white mat cores. In contrast, the orange mat core has relatively high sulfide levels at the surface, consistent with high hydrothermal flow in the mat center. Sulfate is abundant in all three cores, with depletion only occurring at ~32 cm and below in the orange mat core, indicating that hydrothermal circulation contributes to the replenishment of sulfate in surficial sediments (Fig. 2d, Table 1).

Ammonium enrichment in hydrothermal sediments is revealed by the increasing concentrations of ammonium downcore in the orange and white mat cores (Fig. 2e, Table 1). Ammonium concentration increases as temperature increases downcore (Ramírez et al., 2021) and does not correlate with peaks in cell abundance. This suggests that the ammonium measured in our sediments is primarily derived from the thermal degradation of organic matter (Von Damm et al., 1985). Deep in the orange mat core, ammonium concentrations reach ~8 mM (Fig. 2e, Table 1), close to the ~10-15 mM concentrations observed in Guaymas Basin hydrothermal fluids (Von Damm et al., 1985).

Nitrate/nitrite levels are relatively negligible in the deeper portions of the orange and white mat cores, with a rapid increase observed starting at ~13.5 cm depth and continue to increase towards the surface (Fig. 2f, Table 1). Bottom water concentrations of nitrate in Guaymas Basin are up to 50 μM (Winkel et al., 2014). Elevated nitrate levels (~75-250 μM) in mat-covered surficial sediments are at least in part due to damaged *Beggiatoaceae* mats leaking nitrate stored in their vacuoles into surficial sediments (Schutte et al., 2018).

Methane is abundant in all three cores, with similar concentrations in near surface sediments (Fig. 2g, Table 1). Downcore, the impact of hydrothermal activity is observed through the elevated methane concentrations of the orange and white mat cores. High methane concentrations (millimolar) are a characteristic feature of Guaymas Basin hydrothermal sediments, similar to those found at cold seep sites (Welhan, 1988, Song et al., 2021).

Hydrothermal methane in Guaymas Basin unmodified by microbial activity has a $\delta^{13}CH_4$ value of ~42 ‰ (McKay et al. 2016, Song et al. 2021). The preferential oxidation of light methane by methane-oxidizing archaea leads to the orange and white mat cores containing

methane with a heavier carbon isotopic signature (Fig. 2h, Table 1). The lighter carbon isotopic signature of methane throughout the bare sediment core and near the surface of the orange and white mat cores, indicates microbial methanogenesis.

Sequencing Profile. LoopSeq recovered several lineages of anaerobic heterotrophic bacteria that are well established by previous Guaymas Basin sequencing surveys using clone libraries of near full-length 16S rRNA genes (Teske et al., 2002, Dowell et al., 2016, McKay et al., 2016). Additionally, a high proportion of unclassified bacterial diversity is revealed. Sulfur-cycling lineages are particularly well represented in the sequencing profile (Fig. 3). We analyzed the alpha diversity of each mat site using five measures (Observed, Chao1, Shannon, Simpson, and Inverse Simpson) and found no significant difference in alpha diversity across these three sites (Suppl. Fig. 1). We performed phylogenetic analyses on these lineages to determine their intragroup diversity.

Beggiatoaceae. *Beggiatoaceae* are an interesting test of LoopSeq capabilities, as previous attempts to generate full-length sequences from sediment samples have been largely unsuccessful. Currently, existing sequences are derived from cleaned *Beggiatoaceae* filaments (McKay et al., 2012). Due to the size of individual *Beggiatoaceae* cells, they are outnumbered by other much smaller marine bacteria, complicating sequencing efforts and requiring high-throughput methods to overcome the ubiquitous presence of other marine bacterial groups. In our survey, all LoopSeq variants (L-ASV) identified as *Beggiatoaceae* matched reference sequences of the white or orange phylotype, with no additional phylotypes identified (Fig. 4, Suppl. Fig. 2). However, we do not know if sequencing presents a full picture of *Beggiatoaceae* diversity in Guaymas Basin. There is no evidence for introns within the 16S rRNA genes of Guaymas Basin *Beggiatoaceae,* although they have been observed in non-Guaymas Basin *Beggiatoaceae* (Salman et al., 2011). Recovered L-ASVs were generally found to be associated with surficial sediments underlying white and orange *Beggiatoaceae* mats. Some L-ASVs were found deeper below the surface, which can be attributed to the “Smear effect”, when the coring device pulls some of the long filaments down into the sediment column.

***Candidatus* Desulfofervidus.** In contrast to *Beggiatoaceae*, *Candidatus* Desulfofervidus sequences are often recovered in Guaymas Basin sequencing surveys (McKay et al., 2016, Dowell et al., 2016). *Candidatus* Desulfofervidus is a sulfate-reducing syntrophic partner of methane and alkane oxidizing archaea (Laso-Pérez et al., 2016) with a thermal optimum of 50ºC

(Holler et al., 2011) to 60 ºC (Kniemeyer et al., 2007, Wegener et al., 2015). Although often observed as a syntroph, *Ca.* Desulfofervidus can also survive as a free-living hydrogenotroph without methane or alkane oxidizing partners (Krukenberg et al., 2016). *Ca.* Desulfofervidus is a phylogenetically narrow clade, as it is classified as its own family, order, and class-level lineage within the Phylum *Desulfobacterota* (Waite et al., 2020). However, previous research has not examined the phylogenetic diversity within *Ca.* Desulfofervidus.

Our phylogenies identified several monophyletic well-supported clusters, each with nearly identical 16S rRNA gene sequences. Each cluster contained reference sequences from 50ºC (Holler et al., 2011) or 60 ºC (Kniemeyer et al. 2007, Wegener et al., 2015) enrichments. All reference sequences were from Guaymas Basin, with no close matches from other sites. The close alignment of our sequences with established Guaymas Basin reference sequences attests to their quality. Our phylogeny supports the previous assertion of Krukenberg et al. (2016), that all *Ca.* Desulfofervidus lineages are closely related and form a 16S rRNA gene sequence cluster of approximately 98.5 % sequence identity (Suppl. Data File, Sheet 2). The six clusters, supported with bootstrap values ≥ 79 % (Fig. 5), imply the presence of unrecognized species diversity within *Ca.* Desulfofervidus.

We found sequences in GenBank that formed two deeply branching clusters with strong bootstrap support that are distinct from the major group of *Ca.* Desulfofervidus (Fig. 5). These clusters were separated from the main group by sequence distances up to 5.8% (Suppl. Data File, Sheet 2). The recovery of these sequences across independent studies at different vent sites suggests unrecognized microbial diversity related to *Ca.* Desulfofervidus. A previous metagenomic survey of Guaymas Basin hydrothermal sediments detected MAGs (labeled as B74_G16, B4_G9) branching between *Ca.* Desulfofervidus and *Thermodesulfobacteriaceae* (Dombrowski et al., 2018). Detailed analyses of these MAGs would reveal the genomic content and physiological potential of Desulfofervidus-affiliated lineages.

SEEP-SRB2. Like *Ca.* Desulfofervidus, SEEP-SRB2 sequences are often recovered in Guaymas Basin sequencing surveys (Dowell et al., 2016). Our survey recovered sequences from slightly below the surface to approximately 15 cmbsf. Unlike *Ca.* Desulfofervidus, SEEP-SRB2 sequences are recovered from diverse non-hydrothermal environments; cold seeps, salt lakes, coastal sediments, and estuaries (Kleindienst et al., 2012, Ruff et al., 2015). Despite its widespread occurrence and likely ecological importance as a syntrophic partner of methane and

alkane oxidizers (Krukenberg et al., 2018), the internal phylogenetic structure of this group has not been examined in any detail.

Our SEEP-SRB2 phylogeny is largely comprised of a well-supported major cluster with ~97.5% sequence similarity (Suppl. Data File, Sheet 3, equivalent to *Genus* level; Schloss & Handelsman, 2005). Pure culture relatives *Dissulfuribacter thermophilus* and *Dissulfurimicrobium hydrothermale* are thermophilic sulfur disproportionators isolated from hydrothermal environments (Slobodkin et al., 2013, Slobodkin et al., 2016). These pure cultures constitute separate lineages but share a deep branching point with SEEP-SRB2 (Fig. 6). The distinctiveness of these lineages is further supported by sequence distances of up to 11% (Suppl. Data File, Sheet 3). Our 16S rRNA gene sequences reveal that SEEP-SRB2 would form a stand-alone group within *Dissulfuribacteraceae* (Waite et al., 2020). Further phylogenetic diversity that would fall between the pure culture examples (*Dissulfuribacter thermophilus* and *Dissulfurimicrobium hydrothermale*) and SEEP-SRB2 remains to be explored. Previously, the creation of a taxonomic family to comprise *Dissulfuribacter thermophilus* and *Dissulfurimicrobium hydrothermale* has been suggested (Slobodkin et al., 2013). Our phylogenetic trees highlight that such a group would also include SEEP-SRB2 (Fig. 6).

SEEP-SRB4. In contrast to the syntrophic symbionts SEEP-SRB1 and SEEP-SRB2, SEEP-SRB4 has largely been overlooked since it was proposed 20 years ago (Knittel et al., 2003). FISH surveys indicate that SEEP-SRB4 is not a syntroph, but occurs as individual free-living cells (Knittel et al., 2003). The closest cultured relatives of SEEP-SRB4 are non-thermophilic sulfur-disproportionating genera such as *Desulforhopalus* (Isaksen & Teske, 1996), *Desulfocapsa* (Finster et al., 1998), *Desulfofustis* (Friedrich et al., 1996), and the sulfate-reducer, *Desulfotalea* (Knoblauch et al., 1999). While SEEP-SRB2 has been enriched from Guaymas Basin sediments at 37 ºC (Krukenberg et al., 2018), there is currently no evidence that SEEP-SRB4 is moderately thermotolerant. We seek to test this assumption in our survey, checking the distribution of SEEP-SRB4 in surficial hydrothermal sediments. As with SEEP-SRB2, we seek to investigate the previously unrecognized phylogenetic diversity of SEEP-SRB4.

Our SEEP-SRB4 phylogeny depicts one major cluster with strong bootstrap support (100 %) and > 98.9% sequence identity (Suppl. Data File, Sheet 4). This cluster contains several well-supported, phylogenetically narrow clusters (Fig. 7). While the phylogeny shows a potential Guaymas Basin-specific subcluster of four sequences, the rest of the subclusters contain a global

distribution of sequences from cold seep sites and Guaymas Basin.

The majority of L-ASVs for SEEP-SRB4 are retrieved from the top ~6 cm of the sediment across the entire lateral hydrothermal gradient (Suppl. Table 2). The preference for surficial sediments may be due to the abundance of elemental sulfur and polysulfides located there (Teske et al., 2016). A similar preference for surficial sediments with coexisting sulfate and sulfide was noted in the first study of SEEP-SRB4 (Knittel et al., 2003). SEEP-SRB4 bacteria seem to be able to colonize surficial hydrothermal sediments as long as in-situ temperatures remain relatively cool, similar to the strategy utilized by Guaymas Basin *Beggiatoaceae* (McKay et al., 2012).

***Desulfatiglans*.** *Desulfatiglandales* is an order-level lineage within Phylum *Desulfobacterota* that contains polyaromatic degrading organisms, both isolated and uncultured species. The order and family level taxonomy are named after *Desulfatiglans annilini*, the first cultured representative (Suzuki et al., 2014). Sequences related to *Desulfatiglans* are often recovered in Guaymas Basin sequencing surveys (Ramírez et al., 2021, Dowell et al., 2016), including the shallow subsurface (Edgcomb et al., 2022). In contrast to the tightly clustered groups of SEEP-SRB2 and SEEP-SRB4, *Desulfatiglans* exhibits a greater degree of phylogenetic diversity.

Our Guaymas Basin sequences and almost all GenBank sequences were not closely related to cultured isolates that degrade polyaromatic and substituted-aromatic compounds (Fig. 7). Even finding uncultured sequences that were closely related (>98% sequence identity) to some of our Guaymas Basin ASVs proved to be difficult. This could imply an undersampling of the natural diversity of *Desulfatiglans*, or their ongoing diversification and speciation. Previously, *Desulfatiglans* has been classified into two groups distinguished by genomic and physiological differences, Group 1 (sulfate reducers) and Group 2 (subsurface, halophiles) (Jochum et al., 2018). Most of our L-ASVs belong to Group 1 and a few belong to Group 2.

Outside of these two groups, we found two well supported hydrothermal clusters (Fig. 8). The first cluster contained L-ASV 190 (predominately recovered from the white mat site), sequences from 37 ºC and 50 ºC enrichments of Guaymas Basin sediment (Kellermann et al., 2012, Wegener et al., 2015) and an environmental sequence from Guaymas Basin hydrothermal sediment (McKay et al., 2016). The second cluster contained L-ASV 207 (predominately recovered from the orange mat site), a sequence from a *Desulfatiglans* MAG that was prevalent

in a 70 ºC enrichment of Guaymas Basin sediment (Zehnle et al., 2023), and environmental sequences from diverse hydrothermal sediments (Li et al., 2014, Li et al., 2020). We examined these sequences via distance matrix analyses. In our distance matrix analyses we find that these clusters generally separated from other sequences by 11-12% sequence identity (Suppl. Data File, Sheet 5).

In contrast to other sulfate-reducers that occur in warm and hot GB sediments , we observed most of our *Desulfatiglans* L-ASVs in cool sediments, suggesting that they do not depend on methane and light hydrocarbons derived from hydrothermal fluids, and instead utilize polyaromatics (Schnell & Schink, 1991, Zehnle et al., 2023). Polyaromatics from hydrothermal oils are prevalent throughout Guaymas Basin sediments of diverse thermal regimes (Kawka & Simoneit, 1990), and *Desulfatiglans* has evolved to utilize polyaromatics across the thermal spectrum.

Chimera Issues. We found that LoopSeq produced chimeras in the majority of *Candidatus* Desulfofervidus sequences we examined. Segments of these sequences were entered into BLASTn, and we discovered that the chimeras consistently occurred in the first ~200 bp. BLASTn searches of the chimeric segments revealed their relation to other marine sediment bacteria such as *Chloroflexi*. The chimera breaks are located within the highly variable Helix 11 of the 16S rRNA gene (Van de Peer, et al. 1996), and therefore appear to be secondary structure dependent. These issues with *Ca.* Desulfofervidus sequences were observed in samples across the DNA concentration range, from very high (42.4 ng/µl) to very low (0.5 ng/µl). Automated chimera identifying programs can have sensitivity issues when used with uncultured lineages that have poorly resolved phylogenies. We found that trimming off the first ~200 bp remedied the chimera issue, resulting in sequences with high alignment quality and >97% similarity to previously archived *Ca.* Desulfofervidus sequences available in GenBank.

LoopSeq recovered eight sequences identified by the DADA2 annotation pipeline as "*Thermodesulfobacterium*". Initial analysis of theses sequences showed that they were plagued with chimera and artifact issues, a potential consequence of low DNA yields from deep, hot samples. Two sequences were salvaged; one did not have chimera issues (L-ASV 12240), while the other was trimmed to only include the first ~340 bp (L-ASV 11484). These two sequences came from samples with low DNA concentrations (Sample 4872-06-08, 0.5 ng/µl and Sample 4872-6-09, 0.12 ng/µl). These two sequences formed a Guaymas Basin specific cluster (Suppl.

Fig. 3) with the thermophilic ANME-1 syntroph *Thermodesulfobacterium torris* (Benito Merino et al., 2022) and a nearly identical hydrothermal sediment clone (McKay et al., 2016).

Inferred Environmental Constraints. Sequences identified as sulfur-cycling taxa were consistently recovered by LoopSeq, given that there was amplifiable DNA. Sulfur-cycling bacteria of varied taxa are present throughout surficial hydrothermal sediments in the Guaymas Basin. The composition of sulfur-cycling communities shifts along the lateral hydrothermal gradient with increasing temperature, and with sediment depth, as shown in our conceptual model (Fig. 9).

Carbon sources are likely to shift throughout hydrothermal gradients in the sediments. Aromatic hydrocarbons serve as a widely-available carbon source for aromatic-degrading bacteria throughout surficial Guaymas Basin sediments (Mara et al., 2022, Gutierrez et al., 2015, Goetz & Jannasch, 1993). In contrast, alkanes and methane occur are more abundant near hydrothermally active “hot spots” (Song et al., 2021, McKay et al., 2016). The abundance of alkanes and methane in hot sediments contributes to the evolution of thermotolerance and thermophily in several groups of alkane and methane degrading bacteria (Zehnle et al., 2023, Benito Merino et al., 2022). The upper limit of hydrocarbon degradation is approximately 80 ºC, which is supported by the increased abundance of ^{13}C-depleted substrates, which reflects the absence of microbial degradation (Song et al., 2021).

Conclusions. LoopSeq is a promising option for the high throughput long read sequencing of diverse microbial communities in hydrothermal sediments. The huge quantity of sequences yielded by LoopSeq allowed us to further resolve the fine scale phylogenetic structure of sulfur-cycling bacterial groups that are characteristic of Guaymas Basin hydrothermal sediments. The five well-supported clusters revealed in our *Candidatus* Desulfofervidus phylogeny may represent unrecognized physiological and genomic diversity that calls for further investigation beyond the initial description of this group (Krukenberg et al., 2016). Investigating SEEP-SRB2, SEEP-SRB4, and *Ca.* Desulfofervidus showed that they are all phylogenetically distinct groups without a spectrum of close relatives among environmental clones as represented in NCBI GenBank (Figs. 5, 6, & 7). SEEP-SRB2, SEEP-SRB4, and *Ca.* Desulfofervidus all contain considerable internal phylogenetic diversity within their respective clades. Sulfur-disproportionating species and genera are among the closest cultured relatives of SEEP-SRB2 and SEEP-SRB4 (Figs. 6 & 7). In our distance analyses we see sequences distances of up to ~8%

between sulfur-disproportionators and SEEP-SRB2 and up to ~5% between sulfur-disproportionators and SEEP-SRB4 (Suppl. Data File, Sheets 3 & 4). The near-full-length sequences generated by LoopSeq enabled these distance analyses. Elemental sulfur and sulfur species of intermediate oxidation states are abundant at seep sites (Jørgensen et al., 2019). This provides a favorable environment for sulfur-disproportionating bacteria, and the diversification of sulfur-oxidizing and sulfate-reducing bacterial lineages.

However, the chimera issues that we detected in sequences identified as *Ca.* Desulfofervidus, *Thermodesulfobacterium*, and *Beggiatoaceae*, underscore the need for phylogenetic analyses and alignment comparisons with high quality reference sequences to confirm the quality and identity of LoopSeq sequences, and the reliability of microbial community analyses. We also note that our DADA2 analysis of these sequences was not sufficient to detect these chimeras. Without manual verification of sequence alignments and scrutiny of isolated distal branches in phylogenetic clusters, problematic sequences can go undetected, and create artificial diversity. Our observation of lineage-specific chimera issues calls for caution when using LoopSeq alone to investigate extreme and unusual bacterial groups. Since we submitted our samples for sequencing (early 2022), Element Biosciences has instituted some changes with the handling of low-biomass samples (such as our own) has adapted the chemistry of LoopSeq to improve DNA yield in low biomass samples (Element Biosciences representative Dr. Caroline Obert, personal communication). Further protocol development of LoopSeq should keep an eye on this issue, and check sequence accuracy among a wide range of microbial target groups.

LoopSeq has successfully enabled a survey of the diversity of sulfur-cycling bacteria across a thermal and substrate gradient up to the current limit of hydrocarbon degradation. Due to the scope of this study, the diversity of archaea in surficial Guaymas Basin sediments was not investigated with LoopSeq. Further work may use LoopSeq to investigate potentially unknown archaeal diversity in habitats with extreme conditions or along environmental gradients (e.g., Guaymas Basin). Phylogenetic resolution and range of archaeal lineages is limited by sequence coverage. Due to the limitations of popular primers, most available archaeal 16S rRNA gene sequences are 800 bp in length or less (Teske & Sørensen, 2008). High quality near full-length 16S rRNA gene sequence data, such as that provided by LoopSeq, would allow for an improved view of archaeal diversity.

Conflict of Interest Statement. The authors declare that the research was conducted in the absence of any commercial or financial relationships that could be construed as a potential conflict of interest.

Author Contributions. John Hinkle analyzed the sequence data, created the figures, isolated the DNA, and wrote the manuscript. Jeffrey Chanton performed the methane concentration and stable isotope analyses. Molly Moynihan wrote the DADA2 script used to analyze the sequence data. S. Emil Ruff prepared the samples for submission and handled interactions with Element Biosciences over time and advocated on the group's behalf. Andreas Teske obtained the samples during Alvin Dive 4872, guided the interpretation of the phylogenetic trees and geochemical data, supported the development of the manuscript, and taught John Hinkle the DNA extraction method.

Funding. This study was supported by an NSF Biological Oceanography grant to AT (2048489), and by a grant from the Simons Foundation to SER (824763).

Acknowledgements. We thank the R/V *Atlantis* and HOV *Alvin* crews for their exemplary support at sea, especially *Alvin* pilot Jefferson Grau for expert handling of the craft. We thank Chris Chambers for conducting the sulfide analyses, and Eleanor Greene and Hannah Vanderscheuren for clean-up and quantification of the DNA. We thank Element Biosciences for their patience with our complex environmental samples.

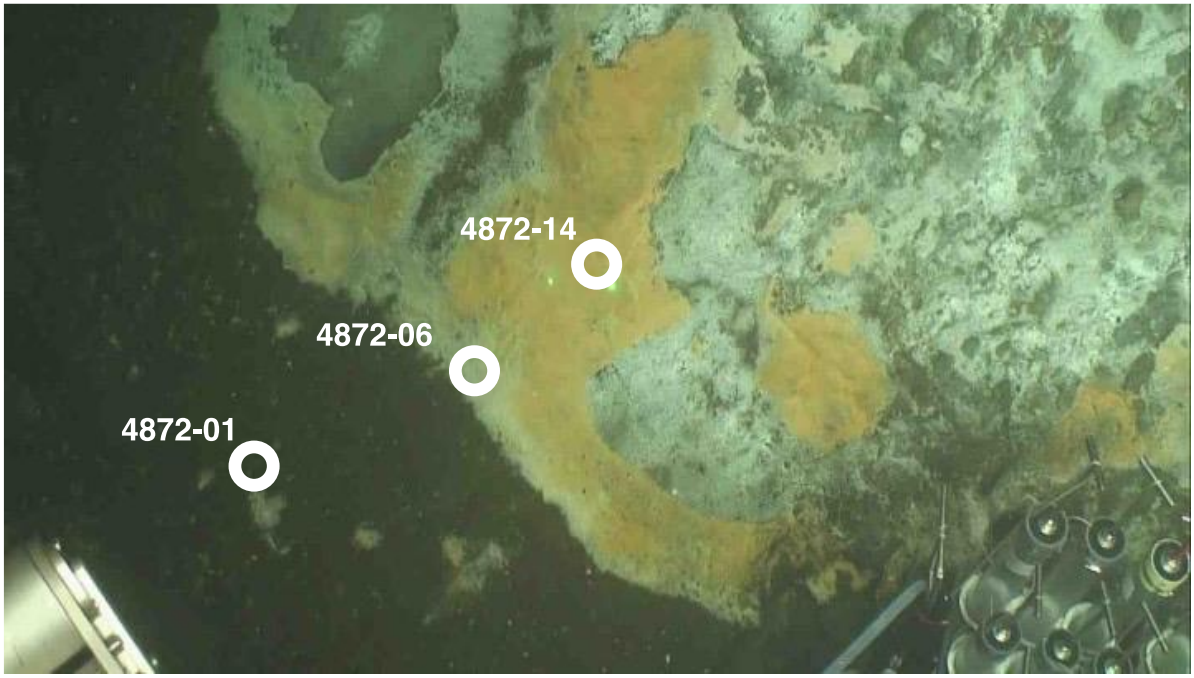

Figure 1. Seafloor image of sampling mat area at Dive 4872. Approximate location of push coring sites are labeled in white. Image courtesy of HOV *Alvin* Dive Team.

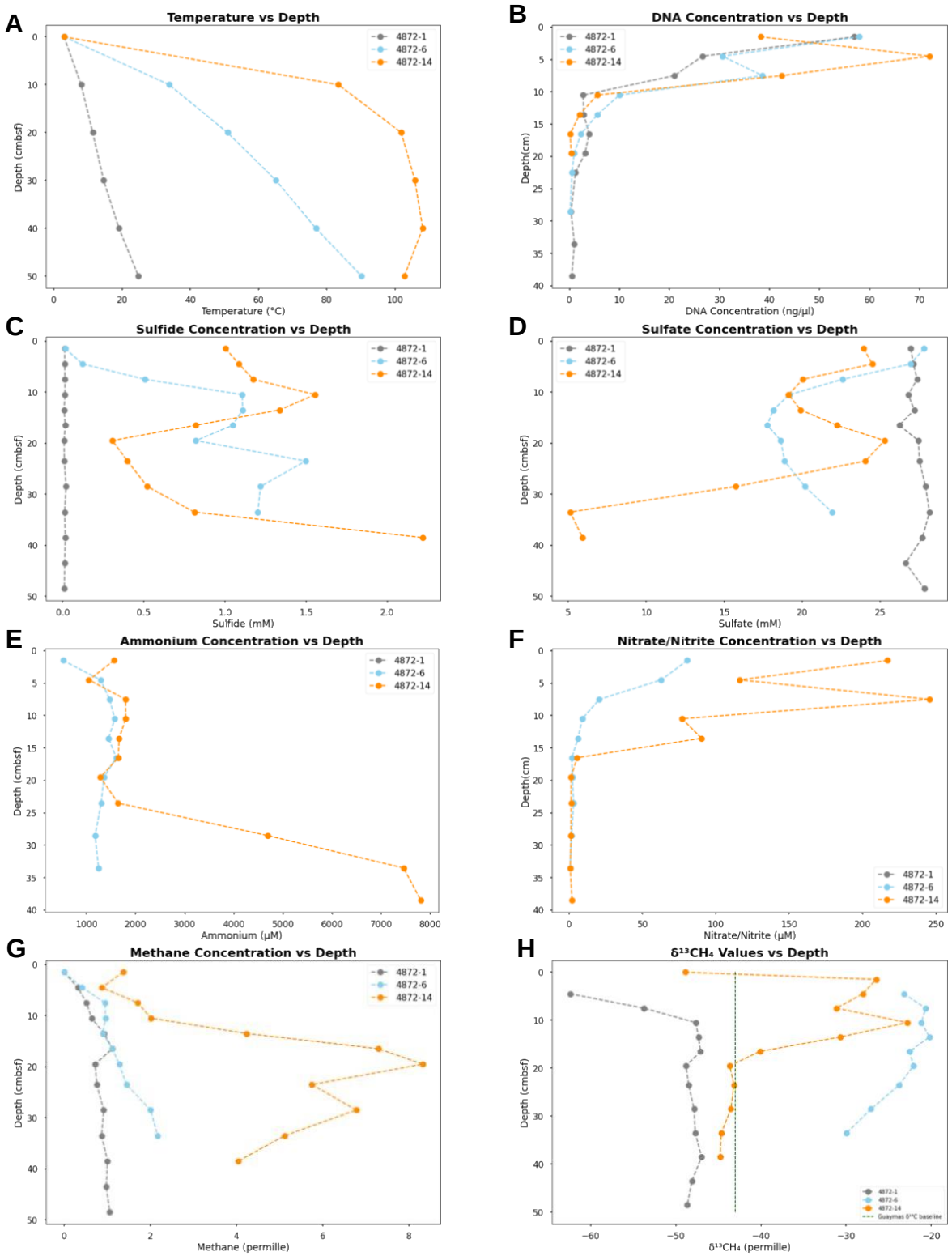

Figure 2. Plots of in-situ temperatures and geochemical parameters for sediment cores. Sulfide, sulfate, Ammonium, and Nitrite/Nitrate concentrations obtained from porewater. Methane concentrations and $\delta^{13}C$ values obtained from whole sediment.

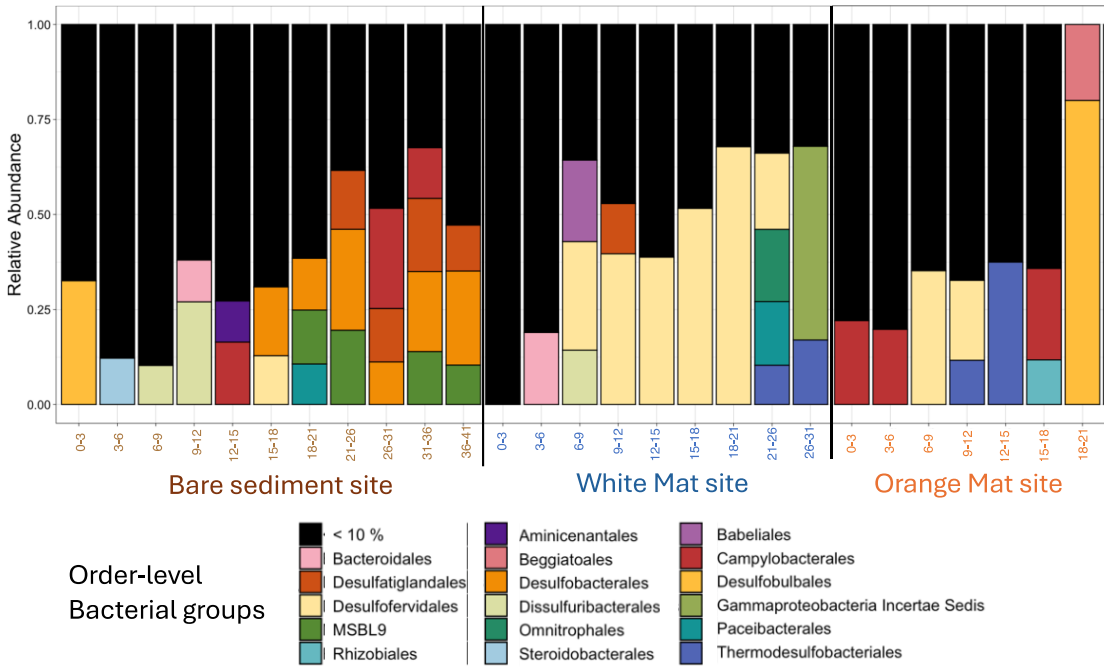

Figure 3. Stacked bar plot of most common order-level bacterial groups as represented by >10% of reads. X-axis represents depth below seafloor (in centimeters) for the three sediments cores across the mat transect (bare sediment, white mat, orange mat).

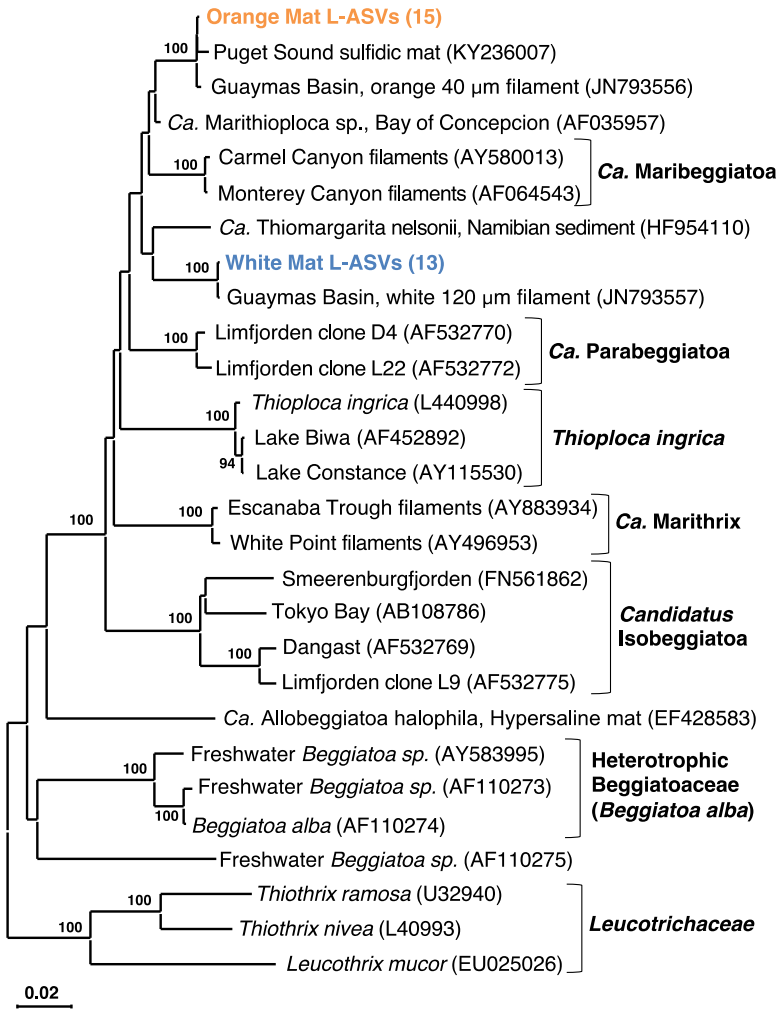

Figure 4. *Beggiatoa* phylogenetic tree. Two distinct clusters are highlighted, 1) an orange filament cluster composed of L-ASVs from the orange mat site (4872-14) and a reference orange filament sequence obtained from GenBank and 2) a cluster composed of L-ASVs from the white mat site (4872-06) and a reference white filament sequence obtained from GenBank. A version of this tree with expanded L-ASV clusters is available as Supplementary Figure 2.

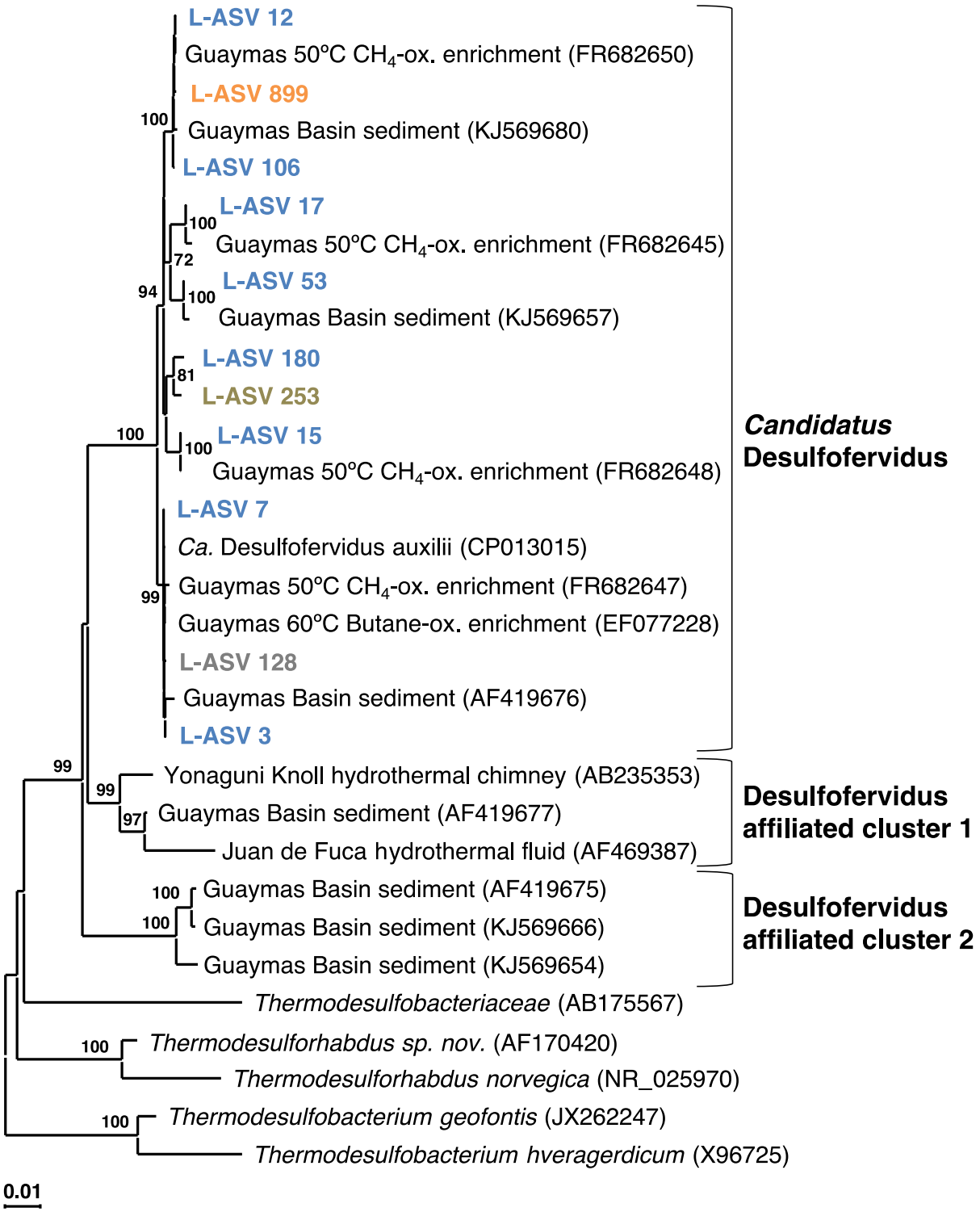

Figure 5. *Candidatus* Desulfofervidus phylogenetic tree L-ASV tip labels are color coded according to the site where the majority (2/3) of reads were recovered. This phylogenetic tree is based on shorter sequences where the first ~200 bp were discarded due to chimera issues. **Brown** = bare sediment, 4872-01; **Blue** = white mat site, 4872-06; **Orange** = orange mat, 4872-14; **Grey** = no site had a 2/3+ share of reads.

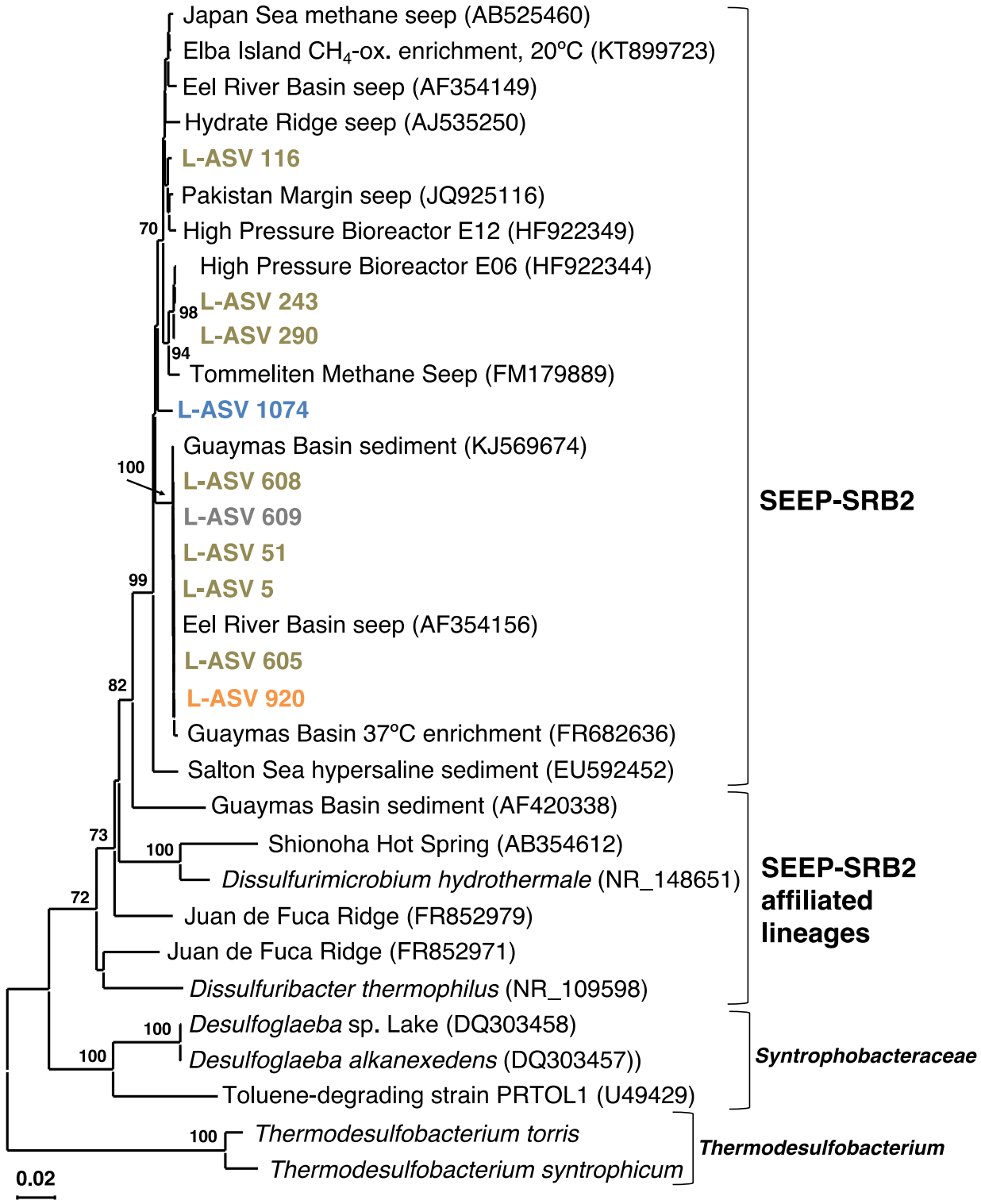

Figure 6. SEEP-SRB2 phylogenetic tree
L-ASV tip labels are color coded according to the site where the majority (2/3) of reads were recovered. This phylogenetic tree is based on shorter sequences where the first ~200 bp were discarded due to chimera issues. **Brown** = bare sediment, 4872-01; **Blue** = white mat site, 4872-06; **Orange** = orange mat,

4872-14; Grey = no site had a 2/3+ share of reads. *Thermodesulfobacterium torris 16S rRNA sequence was obtained from annotated genome (BioSample ID: SAMN27514933).
*Thermodesulfobacterium syntrophicum 16S rRNA sequence was obtained from annotated genome (BioSample ID: SAMN29995626).

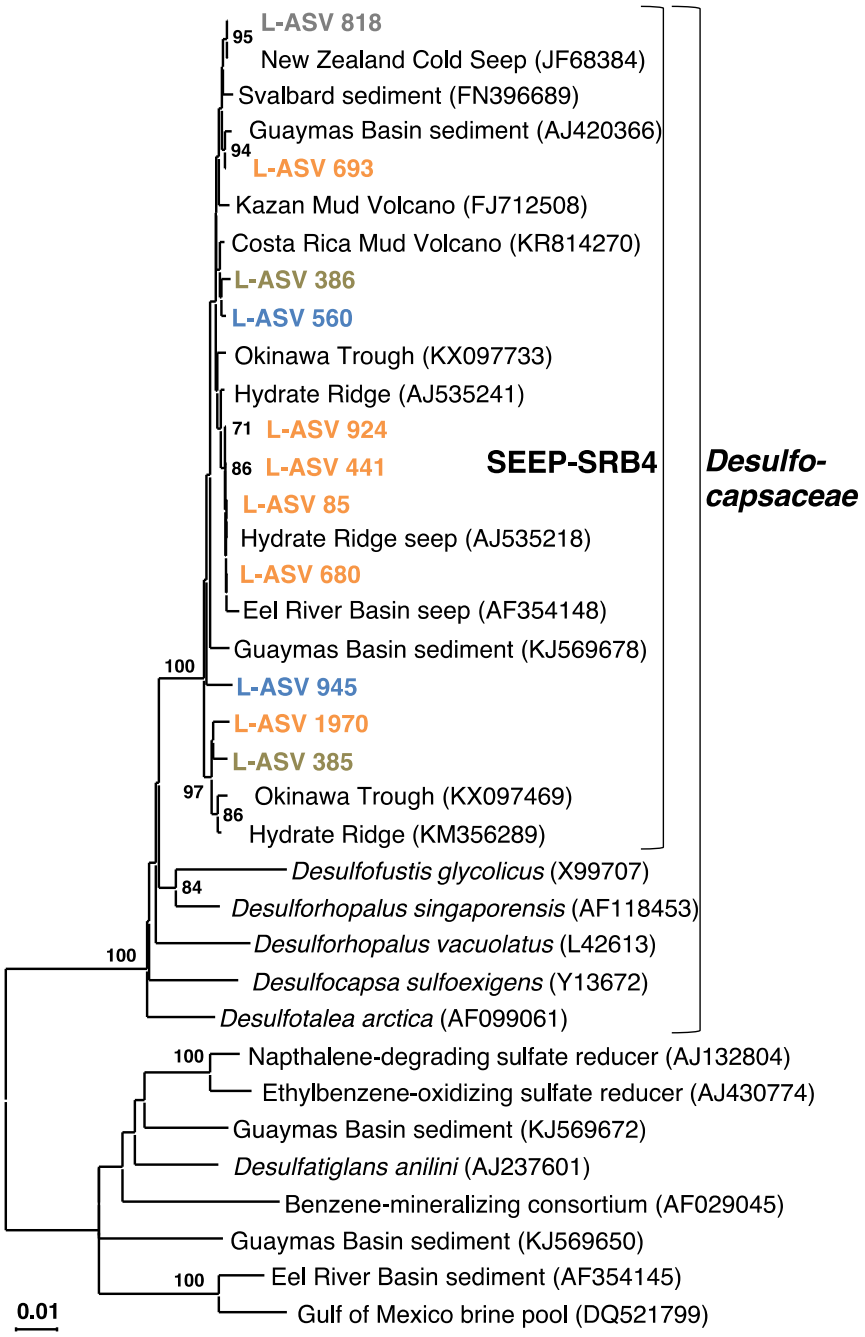

Figure 7. SEEP-SRB4 phylogenetic tree
L-ASV tip labels are color coded according to the site where the majority (2/3) of reads were recovered. This phylogenetic tree is based on shorter sequences where the first ~200 bp were discarded due to chimera issues. **Brown** = bare sediment, 4872-01; **Blue** = white mat site, 4872-06; **Orange** = orange mat, 4872-14; Grey = no site had a 2/3+ share of reads.

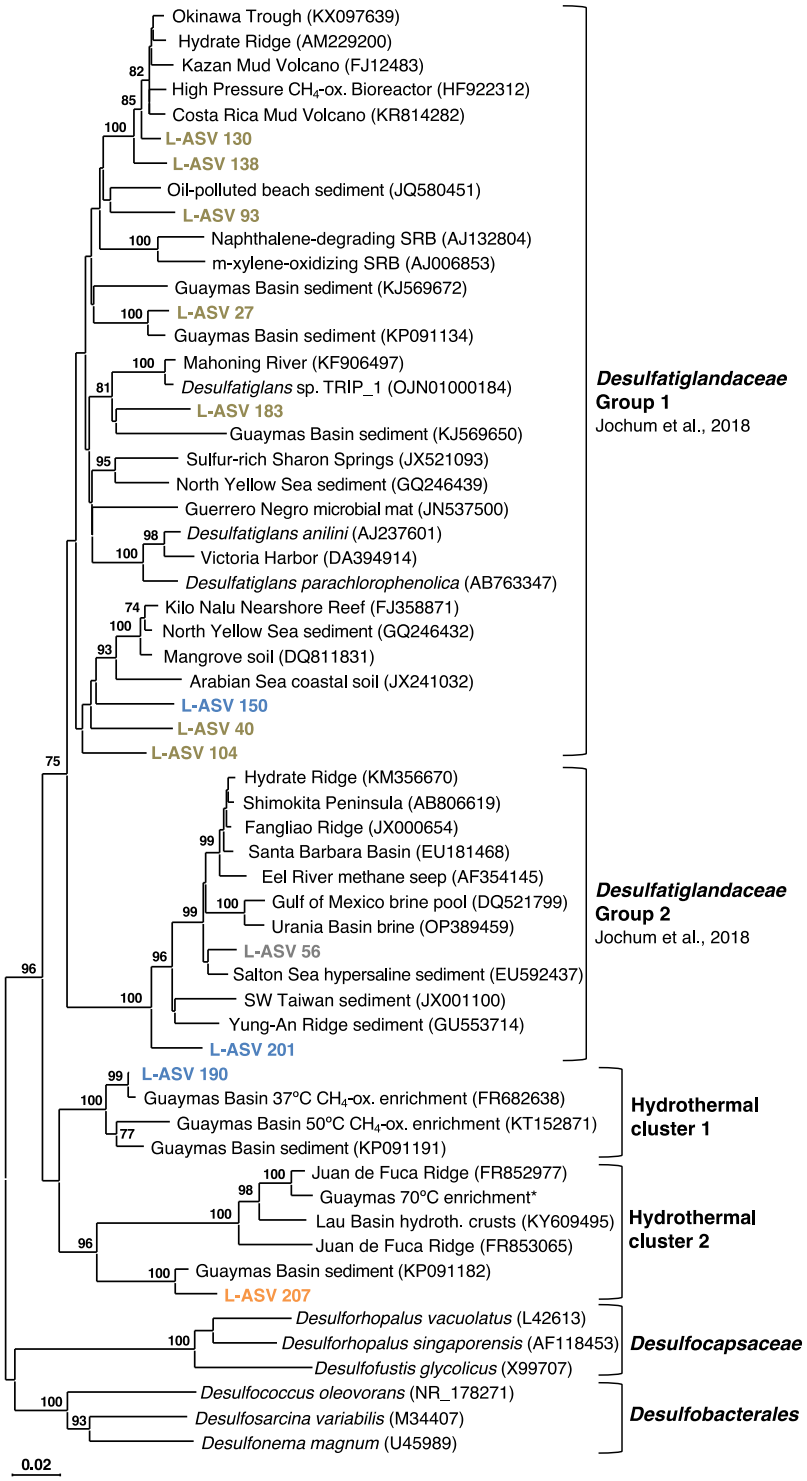

Figure 8. *Desulfatiglans* phylogenetic tree

L-ASV tip labels are color-coded according to the site where the majority (2/3) of reads were recovered. This phylogenetic tree is based on shorter sequences where the first ~200 bp were discarded due to chimera issues. **Brown** = bare sediment, 4872-01; **Blue** = white mat site, 4872-06; **Orange** = orange mat, 4872-14; **Grey** = no site had a 2/3+ share of reads.

*Guaymas 70ºC enrichment sequence is from MAG 9 (B70 culture) under BioProject PRJNA1013425.

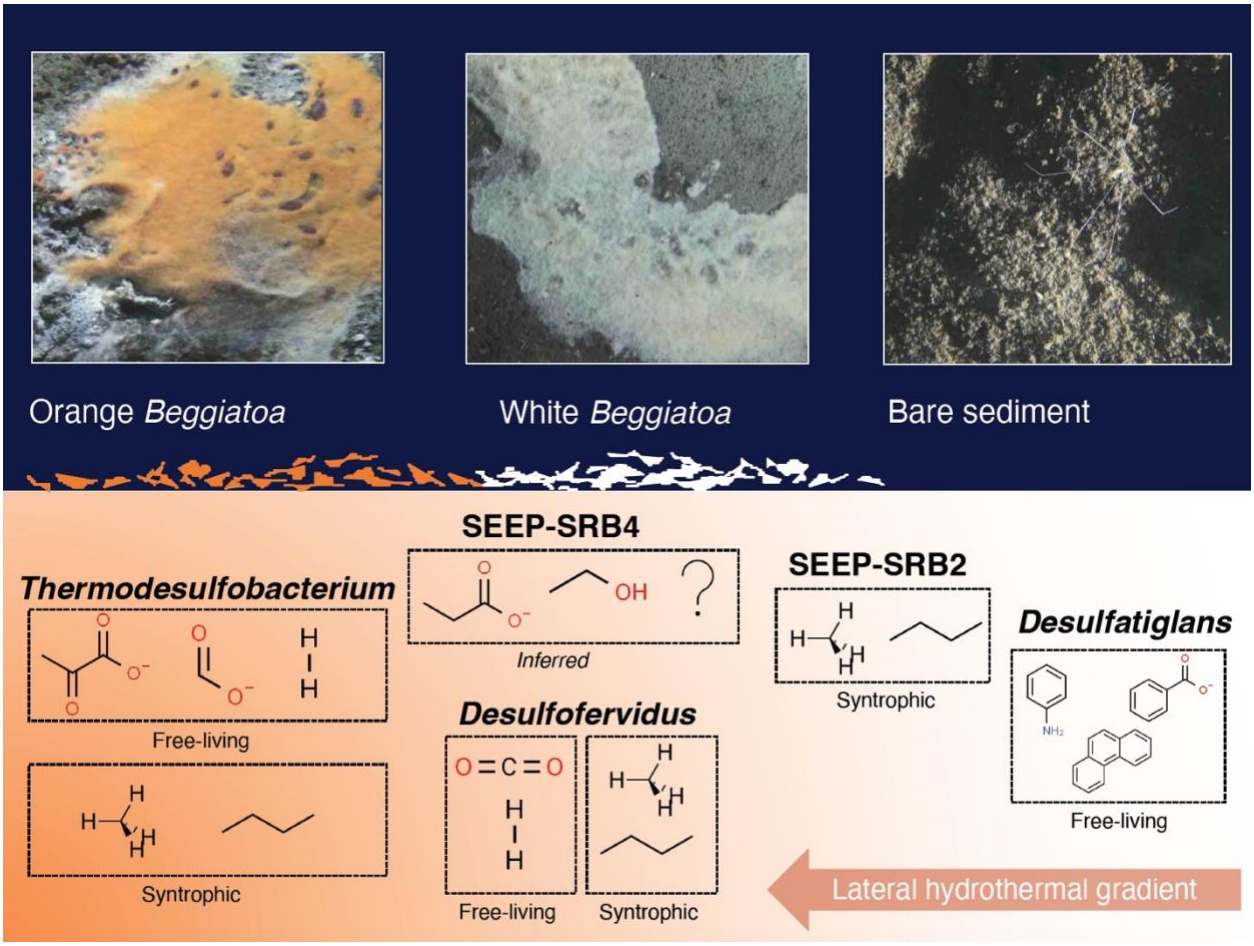

Figure 9. Conceptual figure of sulfur-cycling bacterial groups (with examples of preferred substrates) and their distribution along a lateral hydrothermal gradient in surficial Guaymas Basin sediments. Examples of preferred substrates are shown for both free-living and syntrophic lifestyles, when applicable. Molecular structure images of the preferred substrates were obtained from chemspider.com. *Beggiatoa* and sediment close up images were captured with the bottom facing camera of HOV *Alvin* during Dive 4872.

Depth Range (cm)	Temperature (°C)	Sulfide (mM)	Sulfate (mM)	Ammonium (µM)	Nitrite/Nitrate (µM)	Methane (mM)	δ13C-CH4 (‰)	δ13C-CH4 stdev (‰)
4872-1								
supernatant	3*	0.016	27.42	NA	NA	NA	NA	NA
0-3 cm	3.55^	0.012	26.97	NA	NA	*too low*	NA	NA
3-6	4.86^	0.012	27.13	NA	NA	0.32	-62.40	0.32
6-9	6.17^	0.014	27.37	NA	NA	0.52	-53.73	0.07
9-12 cm	8	0.014	26.800	NA	NA	0.64	-47.64	0.22
12-15 cm	8.78^	0.008	27.190	NA	NA	0.93	-47.34	0.13
15-18 cm	10.1^	0.016	26.230	NA	NA	1.12	-47.09	0.14
18-21 cm	11.4	0.008	27.450	NA	NA	0.72	-48.80	0.16
21-26 cm	13.1^	0.01	27.52	NA	NA	0.76	-48.48	0.15
26-31 cm	14.6	0.02	27.91	NA	NA	0.92	-47.85	0.24
31-36 cm	17.5^	0.012	28.16	NA	NA	0.87	-47.71	0.05
36-41 cm	19.1	0.016	27.71	NA	NA	1.01	-46.97	0.13
41-46 cm	21.9^	0.012	26.63	NA	NA	0.98	-48.11	0.16
46-51 cm	24.8	0.01	27.83	NA	NA	1.06	-48.64	0.01
4872-6								
supernatant	3*	0.014	28.31	182.6	21.70	NA	NA	NA
0-3 cm	24.3^	0.016	27.81	520.4	80.56	NA	NA	NA
3-6 cm	28.4^	0.122	26.94	1285	62.82	0.42	-23.22	0.19
6-9 cm	32.6^	0.507	22.59	1468	20.59	0.95	-20.67	0.11
9-12 cm	33.8	1.106	19.18	1572	8.942	0.96	-21.17	0.00
12-15 cm	40.9^	1.108	18.14	1448	6.150	0.90	-20.23	0.29
15-18 cm	45.1^	1.047	17.77	1601	1.806	1.12	-22.57	0.06
18-21 cm	50.9	0.821	18.63	1352	2.176	1.28	-22.10	0.12
21-26 cm	54.8^	1.497	18.87	1295	3.034	1.45	-23.78	0.14
26-31 cm	65.1	1.218	20.17	1172	1.618	2.01	-27.08	0.08
31-36 cm	68.6^	1.202	21.91	1242	0.6760	2.17	-29.94	0.09
4872-14								
supernatant	3*	0.222	28.68	92.04	20.20	0.73	-48.86	0.15
0-3 cm	80.9^	1.004	23.95	1558	216.8	1.37	-26.49	0.18
3-6 cm	83.3^	1.086	24.50	1046	116.4	0.88	-28.05	0.19
6-9 cm	85.8^	1.173	20.04	1794	245.6	1.71	-31.14	0.06
9-12 cm	83.4	1.556	19.12	1796	77.08	2.02	-22.83	0.12
12-15 cm	90.8^	1.336	19.90	1662	90.24	4.23	-30.70	0.12
15-18 cm	93.3^	0.819	22.23	1643	5.426	7.30	-40.13	0.08
18-21 cm	101.8	0.305	25.28	1279	1.290	8.32	-43.66	0.12
21-26 cm	99.1^	0.399	24.06	1640	1.420	5.75	-43.17	0.04
26-31 cm	105.6	0.521	15.74	4689	1.274	6.78	-43.53	0.08
31-36 cm	107.4^	0.811	5.118	7458	0.7760	5.12	-44.66	0.02
36-41 cm	108.1	2.218	5.921	7808	1.976	4.04	-44.79	0.32

Table 1. Table of in-situ temperatures and geochemical parameters for sediment cores. Sulfide, sulfate, Ammonium, and Nitrite/Nitrate concentrations obtained from porewater. Methane concentrations and $\delta^{13}C$ values obtained from whole sediment.

References

1. Benito Merino, D., Zehnle, H., Teske, A. and Wegener, G., 2022. Deep-branching ANME-1c archaea grow at the upper temperature limit of anaerobic oxidation of methane. *Frontiers in Microbiology*, *13*, p.988871.
2. Callahan, B.J., Grinevich, D., Thakur, S., Balamotis, M.A. and Yehezkel, T.B., 2021. Ultra-accurate microbial amplicon sequencing with synthetic long reads. *Microbiome*, *9*(1), p.130.
3. Callahan, B.J., Grinevich, D., Thakur, S., Balamotis, M.A. and Yehezkel, T.B., 2021. Ultra-accurate microbial amplicon sequencing with synthetic long reads. *Microbiome*, *9*(1), p.130.
4. Callahan, B.J., McMurdie, P.J., Rosen, M.J., Han, A.W., Johnson, A.J.A. and Holmes, S.P., 2016. DADA2: High-resolution sample inference from Illumina amplicon data. *Nature methods*, *13*(7), pp.581-583.
5. Cline, J.D., 1969. Spectrophotometric determination of hydrogen sulfide in natural waters. *Limnology and Oceanography*, *14*(3), pp.454-458.
6. Dombrowski, N., Teske, A.P. and Baker, B.J., 2018. Expansive microbial metabolic versatility and biodiversity in dynamic Guaymas Basin hydrothermal sediments. *Nature communications*, *9*(1), p.4999.
7. Dowell, F., Cardman, Z., Dasarathy, S., Kellermann, M.Y., Lipp, J.S., Ruff, S.E., Biddle, J.F., McKay, L.J., MacGregor, B.J., Lloyd, K.G. and Albert, D.B., 2016. Microbial communities in methane-and short chain alkane-rich hydrothermal sediments of Guaymas Basin. *Frontiers in Microbiology*, *7*, p.17.
8. Edgcomb, V.P., Teske, A.P. and Mara, P., 2022. Microbial hydrocarbon degradation in Guaymas Basin—exploring the roles and potential interactions of fungi and sulfate-reducing bacteria. *Frontiers in microbiology*, *13*, p.831828.
9. Einsele, G., Gieskes, J.M., Curray, J., Moore, D.M., Aguayo, E., Aubry, M.P., Fornari, D., Guerrero, J., Kastner, M., Kelts, K. and Lyle, M., 1980. Intrusion of basaltic sills into highly porous sediments, and resulting hydrothermal activity. *Nature*, *283*(5746), pp.441-445.
10. Felsenstein, J., 1985. Confidence limits on phylogenies: an approach using the bootstrap. *evolution*, *39*(4), pp.783-791.
11. Finster, K., Liesack, W. and Thamdrup, B.O., 1998. Elemental sulfur and thiosulfate disproportionation by Desulfocapsa sulfoexigens sp. nov., a new anaerobic bacterium isolated from marine surface sediment. *Applied and environmental microbiology*, *64*(1), pp.119-125.
12. Goetz, F.E. and Jannasch, H.W., 1993. Aromatic hydrocarbon-degrading bacteria in the petroleum-rich sediments of the Guaymas Basin hydrothermal vent site: preference for aromatic carboxylic acids. *Geomicrobiology Journal*, *11*(1), pp.1-18.
13. Gutierrez, T., Biddle, J.F., Teske, A. and Aitken, M.D., 2015. Cultivation-dependent and cultivation-independent characterization of hydrocarbon-degrading bacteria in Guaymas Basin sediments. *Frontiers in Microbiology*, *6*, p.149000.
14. Holler, T., Widdel, F., Knittel, K., Amann, R., Kellermann, M.Y., Hinrichs, K.U., Teske, A., Boetius, A. and Wegener, G., 2011. Thermophilic anaerobic oxidation of methane by marine microbial consortia. *The ISME journal*, *5*(12), pp.1946-1956.
15. Isaksen, M.F. and Teske, A., 1996. Desulforhopalus vacuolatus gen. nov., sp. nov., a new moderately psychrophilic sulfate-reducing bacterium with gas vacuoles isolated from a temperate estuary. *Archives of microbiology*, *166*, pp.160-168.

16. Jochum, L.M., Schreiber, L., Marshall, I.P., Jørgensen, B.B., Schramm, A. and Kjeldsen, K.U., 2018. Single-cell genomics reveals a diverse metabolic potential of uncultivated Desulfatiglans-related Deltaproteobacteria widely distributed in marine sediment. *Frontiers in microbiology*, *9*, p.384358.
17. Jørgensen, B.B., Findlay, A.J. and Pellerin, A., 2019. The biogeochemical sulfur cycle of marine sediments. Frontiers in microbiology, 10, p.436320.
18. Kawka, O.E. and Simoneit, B.R., 1990. Polycyclic aromatic hydrocarbons in hydrothermal petroleums from the Guaymas Basin spreading center. *Applied Geochemistry*, *5*(1-2), pp.17-27.
19. Kellermann, M.Y., Wegener, G., Elvert, M., Yoshinaga, M.Y., Lin, Y.S., Holler, T., Mollar, X.P., Knittel, K. and Hinrichs, K.U., 2012. Autotrophy as a predominant mode of carbon fixation in anaerobic methane-oxidizing microbial communities. *Proceedings of the National Academy of Sciences*, *109*(47), pp.19321-19326.
20. Kleindienst, S., Herbst, F.A., Stagars, M., Von Netzer, F., Von Bergen, M., Seifert, J., Peplies, J., Amann, R., Musat, F., Lueders, T. and Knittel, K., 2014. Diverse sulfate-reducing bacteria of the Desulfosarcina/Desulfococcus clade are the key alkane degraders at marine seeps. *The ISME journal*, *8*(10), pp.2029-2044.
21. Kniemeyer, O., Musat, F., Sievert, S.M., Knittel, K., Wilkes, H., Blumenberg, M., Michaelis, W., Classen, A., Bolm, C., Joye, S.B. and Widdel, F., 2007. Anaerobic oxidation of short-chain hydrocarbons by marine sulphate-reducing bacteria. *Nature*, *449*(7164), pp.898-901.
22. Knittel, K., Boetius, A., Lemke, A., Eilers, H., Lochte, K., Pfannkuche, O., Linke, P. and Amann, R., 2003. Activity, distribution, and diversity of sulfate reducers and other bacteria in sediments above gas hydrate (Cascadia margin, Oregon). *Geomicrobiology Journal*, *20*(4), pp.269-294.
23. Knoblauch, C., Sahm, K. and Jørgensen, B.B., 1999. Psychrophilic sulfate-reducing bacteria isolated from permanently cold Arctic marine sediments: description of Desulfofrigus oceanense gen. nov., sp. nov., Desulfofrigus fragile sp. nov., Desulfofaba gelida gen. nov., sp. nov., Desulfotalea psychrophila gen. nov., sp. nov. and Desulfotalea arctica sp. nov. *International Journal of Systematic and Evolutionary Microbiology*, *49*(4), pp.1631-1643.
24. Krukenberg, V., Harding, K., Richter, M., Glöckner, F.O., Gruber-Vodicka, H.R., Adam, B., Berg, J.S., Knittel, K., Tegetmeyer, H.E., Boetius, A. and Wegener, G., 2016. Candidatus Desulfofervidus auxilii, a hydrogenotrophic sulfate-reducing bacterium involved in the thermophilic anaerobic oxidation of methane. *Environmental microbiology*, *18*(9), pp.3073-3091.
25. Krukenberg, V., Riedel, D., Gruber-Vodicka, H.R., Buttigieg, P.L., Tegetmeyer, H.E., Boetius, A. and Wegener, G., 2018. Gene expression and ultrastructure of meso-and thermophilic methanotrophic consortia. *Environmental microbiology*, *20*(5), pp.1651-1666.
26. Lagostina, L., Frandsen, S., MacGregor, B.J., Glombitza, C., Deng, L., Fiskal, A., Li, J., Doll, M., Geilert, S., Schmidt, M. and Scholz, F., 2021. Interactions between temperature and energy supply drive microbial communities in hydrothermal sediment. *Communications Biology*, *4*(1), p.1006.
27. Laso-Pérez, R., Wegener, G., Knittel, K., Widdel, F., Harding, K.J., Krukenberg, V., Meier, D.V., Richter, M., Tegetmeyer, H.E., Riedel, D. and Richnow, H.H., 2016.

Thermophilic archaea activate butane via alkyl-coenzyme M formation. *Nature*, *539*(7629), pp.396-401.

28. Li, J., Su, L., Wang, F., Yang, J., Gu, L., Sun, M., Li, Q., Zhou, H. and Fang, J., 2020. Elucidating the biomineralization of low-temperature hydrothermal precipitates with varying Fe, Si contents: Indication from ultrastructure and microbiological analyses. *Deep Sea Research Part I: Oceanographic Research Papers*, *157*, p.103208.
29. Li, J., Zhou, H., Fang, J., Sun, Y. and Dasgupta, S., 2014. Microbial distribution in different spatial positions within the walls of a black sulfide hydrothermal chimney. *Marine Ecology Progress Series*, *508*, pp.67-85.
30. Lizarralde, D., Soule, S.A., Seewald, J.S. and Proskurowski, G., 2011. Carbon release by off-axis magmatism in a young sedimented spreading centre. *Nature geoscience*, *4*(1), pp.50-54.
31. Mara, P., Nelson, R.K., Reddy, C.M., Teske, A. and Edgcomb, V.P., 2022. Sterane and hopane biomarkers capture microbial transformations of complex hydrocarbons in young hydrothermal Guaymas Basin sediments. *Communications Earth & Environment*, *3*(1), p.250.
32. McKay, L., Klokman, V.W., Mendlovitz, H.P., LaRowe, D.E., Hoer, D.R., Albert, D., Amend, J.P. and Teske, A., 2016. Thermal and geochemical influences on microbial biogeography in the hydrothermal sediments of Guaymas Basin, Gulf of California. *Environmental microbiology reports*, *8*(1), pp.150-161.
33. McKay, L.J., MacGregor, B.J., Biddle, J.F., Albert, D.B., Mendlovitz, H.P., Hoer, D.R., Lipp, J.S., Lloyd, K.G. and Teske, A.P., 2012. Spatial heterogeneity and underlying geochemistry of phylogenetically diverse orange and white Beggiatoa mats in Guaymas Basin hydrothermal sediments. *Deep Sea Research Part I: Oceanographic Research Papers*, *67*, pp.21-31.
34. Meyer, S., Wegener, G., Lloyd, K.G., Teske, A., Boetius, A. and Ramette, A., 2013. Microbial habitat connectivity across spatial scales and hydrothermal temperature gradients at Guaymas Basin. *Frontiers in microbiology*, *4*, p.51282.
35. Møller, M.H., Glombitza, C., Lever, M.A., Deng, L., Morono, Y., Inagaki, F., Doll, M., Su, C.C. and Lomstein, B.A., 2018. D: L-amino acid modeling reveals fast microbial turnover of days to months in the subsurface hydrothermal sediment of Guaymas Basin. *Frontiers in microbiology*, *9*, p.967.
36. Ramírez, G.A., Mara, P., Sehein, T., Wegener, G., Chambers, C.R., Joye, S.B., Peterson, R.N., Philippe, A., Burgaud, G., Edgcomb, V.P. and Teske, A.P., 2021. Environmental factors shaping bacterial, archaeal and fungal community structure in hydrothermal sediments of Guaymas Basin, Gulf of California. *PLoS One*, *16*(9), p.e0256321.
37. Ruff, S.E., Biddle, J.F., Teske, A.P., Knittel, K., Boetius, A. and Ramette, A., 2015. Global dispersion and local diversification of the methane seep microbiome. *Proceedings of the National Academy of Sciences*, *112*(13), pp.4015-4020.
38. Ruff, S.E., Biddle, J.F., Teske, A.P., Knittel, K., Boetius, A. and Ramette, A., 2015. Global dispersion and local diversification of the methane seep microbiome. *Proceedings of the National Academy of Sciences*, *112*(13), pp.4015-4020.
39. Rzhetsky, A. and Nei, M., 1995. Tests of applicability of several substitution models for DNA sequence data. *Molecular Biology and Evolution*, *12*(1), pp.131-151.
40. Salman, V., Amann, R., Girnth, A.C., Polerecky, L., Bailey, J.V., Høgslund, S., Jessen, G., Pantoja, S. and Schulz-Vogt, H.N., 2011. A single-cell sequencing approach to the

classification of large, vacuolated sulfur bacteria. *Systematic and applied microbiology*, *34*(4), pp.243-259.

41. Schloss, P.D. and Handelsman, J., 2005. Introducing DOTUR, a computer program for defining operational taxonomic units and estimating species richness. *Applied and environmental microbiology*, *71*(3), pp.1501-1506.
42. Schnell, S. and Schink, B., 1991. Anaerobic aniline degradation via reductive deamination of 4-aminobenzoyl-CoA in Desulfobacterium anilini. *Archives of Microbiology*, *155*, pp.183-190.
43. Schutte, C.A., Teske, A., MacGregor, B.J., Salman-Carvalho, V., Lavik, G., Hach, P. and de Beer, D., 2018. Filamentous giant Beggiatoaceae from the Guaymas Basin are capable of both denitrification and dissimilatory nitrate reduction to ammonium. *Applied and environmental microbiology*, *84*(15), pp.e02860-17.
44. Slobodkin, A.I., Reysenbach, A.L., Slobodkina, G.B., Kolganova, T.V., Kostrikina, N.A. and Bonch-Osmolovskaya, E.A., 2013. Dissulfuribacter thermophilus gen. nov., sp. nov., a thermophilic, autotrophic, sulfur-disproportionating, deeply branching deltaproteobacterium from a deep-sea hydrothermal vent. *International journal of systematic and evolutionary microbiology*, *63*(Pt_6), pp.1967-1971.
45. Slobodkin, A.I., Slobodkina, G.B., Panteleeva, A.N., Chernyh, N.A., Novikov, A.A. and Bonch-Osmolovskaya, E.A., 2016. Dissulfurimicrobium hydrothermale gen. nov., sp. nov., a thermophilic, autotrophic, sulfur-disproportionating deltaproteobacterium isolated from a hydrothermal pond. *International Journal of Systematic and Evolutionary Microbiology*, *66*(2), pp.1022-1026.
46. Sogin, M.L., Morrison, H.G., Huber, J.A., Welch, D.M., Huse, S.M., Neal, P.R., Arrieta, J.M. and Herndl, G.J., 2006. Microbial diversity in the deep sea and the underexplored "rare biosphere". *Proceedings of the National Academy of Sciences*, *103*(32), pp.12115-12120.
47. Song, M., Schubotz, F., Kellermann, M.Y., Hansen, C.T., Bach, W., Teske, A.P. and Hinrichs, K.U., 2021. Formation of ethane and propane via abiotic reductive conversion of acetic acid in hydrothermal sediments. *Proceedings of the National Academy of Sciences*, *118*(47), p.e2005219118.
48. Stecher, G., Tamura, K. and Kumar, S., 2020. Molecular evolutionary genetics analysis (MEGA) for macOS. *Molecular biology and evolution*, *37*(4), pp.1237-1239.
49. Su et al., 2023
50. Suzuki, D., Li, Z., Cui, X., Zhang, C. and Katayama, A., 2014. Reclassification of Desulfobacterium anilini as Desulfatiglans anilini comb. nov. within Desulfatiglans gen. nov., and description of a 4-chlorophenol-degrading sulfate-reducing bacterium, Desulfatiglans parachlorophenolica sp. nov. *International journal of systematic and evolutionary microbiology*, *64*(Pt_9), pp.3081-3086.
51. Teske, A. and Sørensen, K.B., 2008. Uncultured archaea in deep marine subsurface sediments: have we caught them all?. The ISME journal, 2(1), pp.3-18.
52. Teske, A., Hinrichs, K.U., Edgcomb, V., de Vera Gomez, A., Kysela, D., Sylva, S.P., Sogin, M.L. and Jannasch, H.W., 2002. Microbial diversity of hydrothermal sediments in the Guaymas Basin: evidence for anaerobic methanotrophic communities. *Applied and environmental microbiology*, *68*(4), pp.1994-2007.
53. Teske, A., Hinrichs, K.U., Edgcomb, V., de Vera Gomez, A., Kysela, D., Sylva, S.P., Sogin, M.L. and Jannasch, H.W., 2002. Microbial diversity of hydrothermal sediments in

the Guaymas Basin: evidence for anaerobic methanotrophic communities. *Applied and Environmental Microbiology*, *68*(4), pp.1994-2007.

54. Teske, A., McKay, L.J., Ravelo, A.C., Aiello, I., Mortera, C., Núñez-Useche, F., Canet, C., Chanton, J.P., Brunner, B., Hensen, C. and Ramírez, G.A., 2019. Characteristics and evolution of sill-driven off-axis hydrothermalism in Guaymas Basin–the Ringvent site. *Scientific Reports*, *9*(1), p.13847.
55. Teske, A., Wegener, G., Chanton, J.P., Hoer, D., de Beer, D., Zhuang, G., Saxton, M.A., Joye, S.B., Soule, S.A. and Ruff, S.E., 2021. Microbial communities under distinct thermal and geochemical regimes in axial and off-axis sediments of Guaymas Basin. *Frontiers in microbiology*, *12*, p.633649.
56. Van de Peer, Y., Chapelle, S. and De Wachter, R., 1996. A quantitative map of nucleotide substitution rates in bacterial rRNA. *Nucleic acids research*, *24*(17), pp.3381-3391.
57. Von Damm, K.L., Edmond, J.T., Measures, C.I. and Grant, B., 1985. Chemistry of submarine hydrothermal solutions at Guaymas Basin, Gulf of California. *Geochimica et Cosmochimica Acta*, *49*(11), pp.2221-2237.
58. Waite, D.W., Chuvochina, M., Pelikan, C., Parks, D.H., Yilmaz, P., Wagner, M., Loy, A., Naganuma, T., Nakai, R., Whitman, W.B. and Hahn, M.W., 2020. Proposal to reclassify the proteobacterial classes Deltaproteobacteria and Oligoflexia, and the phylum Thermodesulfobacteria into four phyla reflecting major functional capabilities. *International Journal of Systematic and Evolutionary Microbiology*, *70*(11), pp.5972-6016.
59. Wegener, G., Krukenberg, V., Riedel, D., Tegetmeyer, H.E. and Boetius, A., 2015. Intercellular wiring enables electron transfer between methanotrophic archaea and bacteria. *Nature*, *526*(7574), pp.587-590.
60. Welhan, J.A., 1988. Origins of methane in hydrothermal systems. Chemical Geology, 71(1-3), pp.183-198.
61. Winkel, M., de Beer, D., Lavik, G., Peplies, J. and Mußmann, M., 2014. Close association of active nitrifiers with B eggiatoa mats covering deep-sea hydrothermal sediments. *Environmental microbiology*, *16*(6), pp.1612-1626.
62. Zehnle, H., Otersen, C., Benito Merino, D. and Wegener, G., 2023. Potential for the anaerobic oxidation of benzene and naphthalene in thermophilic microorganisms from the Guaymas Basin. *Frontiers in Microbiology*, *14*, p.1279865.
63. Zhou, J., Bruns, M.A. and Tiedje, J.M., 1996. DNA recovery from soils of diverse composition. *Applied and environmental microbiology*, *62*(2), pp.316-322.